Solvent Retention, Thermodynamics, Rheology and Small Angle X-ray Scattering Studies on Thermoreversible Poly(vinylidene fluoride) Gels

ARTICLE *in* THE JOURNAL OF PHYSICAL CHEMISTRY B · SEPTEMBER 2010

Impact Factor: 3.3 · DOI: 10.1021/jp105018h · Source: PubMed

Solvent Retention, Thermodynamics, Rheology and Small Angle X-ray Scattering Studies on Thermoreversible Poly(vinylidene fluoride) Gels

P. Jaya Prakash Yadav, A. K. Patra, P. U. Sastry, Binay. K. Ghorai, and Pralay Maiti*

School of Materials Science and Technology, Institute of Technology, Banaras Hindu University, Varanasi 221 005, India, Solid State Physics Division, Bhabha Atomic Research Centre, Trombay, Mumbai 400 085, India, and Department of Chemistry, Bengal Engineering and Science University, Shibpur, Howrah - 711 103, India

Received: June 01, 2010; Revised Manuscript Received: July 05, 2010

Solvent retention power of poly(vinylidene fluoride) (PVDF) gels has been studied for various homologues of phthalate (aromatic diesters). The thermal stability has been examined for gels of varying morphology. Solvent evaporation, gelation, gel melting, and polymer degradation temperatures have increased with increasing aliphatic chain length of phthalates. The thermodynamics and polymer−solvent compound formations in the PVDF−phthalate gels have been explored. The weight fraction of polymer in compound has decreased with increasing aliphatic chain length. SAXS studies have confirmed the lamellar organization inside the fibrils, and interlamellar distance increases with aliphatic chain length of diesters. The scattering patterns follow the power law behavior ($I(q) \approx q^{-\alpha}$), and polymer gels consist of high-density mass (fibril), voids, and interlamellar region. Dynamic mechanical properties indicate the splintering and reformation of network structure in gels whose percolation frequency has reduced for higher aliphatic chain length phthalate. Morphology-dependent moduli have been observed, and greater mechanical strength has been verified for thicker fibrillar gels both for steady and dynamic measurements.

Introduction

Thermoreversible gelation of synthetic polymers is being studied extensively because of scientific and wide range of technological uses.[1−7] It is important to know the physicochemical processes involved during gelation.[8,9] Polymer gels possess propensity of forming polymer−solvent compounds in a variety of solvents.[10−12] There are few reports of thermoreversible gelation of poly(vinylidene fluoride) (PVDF) in different solvents, and the first report was with γ-butyrolactone.[13] One critical phenomena of gel is its solvent retention power, where <5 wt % of polymer can seize 95% of solvent to make a semisolid material. Gel may loose its solvent under thermal treatment. So far, there is no systematic report of solvent retention power of gel while undergoing heat treatment. Furthermore, the thermodynamic study of PVDF gel is an important area that sheds light on the molecular level information of polymer−solvent complexes. Different molecular weights of PVDF gelation have been studied in different solvents.[14] Therefore, there are changes in structural, morphological, and thermodynamical parameters with varying molecular weight, solvent, temperature, and so on. The PVDF gels melting and gelation temperature has been studied with varying intermittent chain length of aliphatic diesters [$(CH_2)_n$-$(COOEt)_2$].[15] Gelation mechanism, phase diagram, thermodynamics, and polymer−solvent interactions of PVDF gels have been reported for selective solvents.[15−17] A miscible blend of PVDF and PMA in diethyl azelate has been studied on gelation mechanism, morphology, and polymer−solvent compound formation. Mechanical properties for thermoreversible gels have been studied as a function of temperature and limited frequency range.[18,19] The details of PVDF−ethylene carbonate gels have been measured by Dasgupta et al.[20] The dynamic mechanical properties have also been measured for poly(vinylidene fluoride-*co*-hexafluoro propylene) gels in aromatic diesters (phthalates) [Ph-$(COOC_nH_{2n+1})_2$].[21] Recently, we have reported preliminary gelation behavior, morphology, and microstructure of PVDF in aromatic diesters (phthalates) with varying aliphatic chain length.[22] PVDF gels produce the fibrillar morphology and often possess a 3D network structure made up of an array of fibrils in different polymer−solvent complexation.[14,15,17,22,23] Small-angle X-ray scattering (SAXS) can estimate the nature of crystallites distributed and the information about the cross-sectional radius of gyration of the crystallite of gel to assess the domain size of the physical junctions. The scattering pattern usually follows the power-law behavior [$I(q) \approx q^{-\alpha}$], where, $I(q)$ is scattering intensity and q is the wavevector ($= 4\pi/\lambda \sin \theta$).[21,24−27] The structural studies on local scale using SAXS can be supplemented with rheological properties of the gels. If the peak so arises in the scattering pattern, then the interlamellar spacing can be calculated from Bragg's peak $d = 2\pi/q_m$, where q_m is the wavevector corresponding to the maximum peak intensity.

In this work, we report the solvent retention power of PVDF gels in a series of aromatic diesters with varying aliphatic chain length. The effect of morphological changes arising in the presence of different homologues of phthalate on thermal behavior/solvent preservation ability has been elucidated. The variation of aliphatic chain length on gelation temperature and gel melting behavior has been discussed in detail. Thermodynamic aspects, for example, compound formation and phase diagram including the influence of solvent have been studied. We have illustrated PVDF gels with various phthalates to know the insight into morphological patterns by using SAXS. The mechanical strength of PVDF gels both in steady state and dynamic behavior has been worked out and was correlated with their morphological development in different phthalates.

* To whom correspondence should be addressed. E-mail: pmaiti.mst@itbhu.ac.in.

10.1021/jp105018h
Published on Web 08/17/2010

Experimental Section

Materials. A series of phthalates with varying aliphatic chain lengths were used with the general chemical formula of $Ph(COOC_nH_{2n+1})_2$, where n was varied from 1 to 8. Dimethyl phthalate (DMP) and diethyl phthalates (DEP) received from Loba Chemie, dibutyl phthalate (DBP) and dioctyl phthalate (DOP) received from Merck, and dipropyl phthalate (DPP) and dihexyl phthalate (DHP) received from National Chemicals, India were used as received. The n will often be termed as aliphatic chain length, for example, DMP ($n = 1$), DEP ($n = 2$), DPP ($n = 3$), DBP ($n = 4$), DHP ($n = 6$), and DOP ($n = 8$) in the text. PVDF (SOLEF 6008, Ausimont, Italy) of MFI 24 g/10 min (230 °C, 5 kg) was used in this work.

Gel and Dried Gel Preparation. For the preparation of gel, the predetermined amount of PVDF was dissolved in solvent at 200 °C to make a homogeneous solution and then quickly transferred to a fixed temperature liquid bath and until the solution completely froze. The time required to seize flow was considered as the gelation time. The experiment was repeated three times, and an average gelation time (t_{gel}) was calculated for every system at different concentrations. The gelation rate (t_{gel}^{-1}) was calculated from the inverse of gelation time measured. For the preparation of dried gels, PVDF gels in phthalate were immersed in cyclohexane in a Petri dish at room temperature to replace phthalates gradually by low boiling cyclohexane. Cyclohexane was replaced by a fresh set to achieve the replacement equilibrium at a faster rate every 12 h. This process was repeated for 10 days for complete removal of phthalates from gels. After cyclohexane was decanted, resulting gels were initially dried at room temperature, followed by drying under reduced pressure at ambient temperature for 3 days to keep the morphology intact.[22]

Thermal Decomposition. Thermal decompositions of PVDF gels in various phthalates (10 wt % (w/v)) were examined by the use of a thermogravimetric analyzer (TGA) (Mettler-Toledo) fitted with a differential thermal analyzer (DTA). Data were taken from 40−600 °C. All experiments were performed using the heating rate at 10 °C min^{-1} in a nitrogen atmosphere.

Differential Scanning Calorimetry. A small amount of PVDF gel samples was heated at the scan rate of 10 °C/min on a Mettler 832 DSC instrument. The peak temperatures and the enthalpies of fusion were measured from the endotherms using a computer attached with the instrument. After the first melting, the gels were cooled at a constant rate of 10 °C/min to find the gelation temperature, and the heats of gelation were measured in a similar manner. Furthermore, a second heating was taken to ensure the amount of crystallinity/heat of gelation and gel melting temperature after the formation of gel in a controlled cooling environment. The DSC was calibrated with zinc and indium before using the instrument.

Morphology. The morphology of PVDF dried gels (10% (w/v)) was investigated by the use of both a scanning electron microscope (SEM) and a transmission electron microscope (TEM) to observe the distribution of fibril diameter and lateral dimension. PVDF dried gel samples were coated with gold before observation by means of sputtering unit for SEM study in a LEO 435VP instrument operated at 10 kV. We performed the TEM study by pouring 10% (w/v) solution of PVDF in phthalates on a carbon-coated grid, followed by drying at 50 °C under vacuum for 7 days. The morphology of the gel was observed in a TEM (Technai G^2) operated at 100 kV.

Small-Angle X-ray Scattering. SAXS measurements were performed on dried gels using the small-angle goniometer mounted on the 12 kW Rigaku rotating anode X-ray generator with Cu Kα radiation. The intensities were measured by transmission method using a scintillation counter system with pulse height analyzer. Scattered intensities $I(q)$ from each of the four samples were recorded in steps of the scattering angle 2θ, yielding a scattering vector in the range $q = 0.04$ to 1.7 nm^{-1}, where $q = 4\pi/\lambda \sin\theta$ and λ (= 1.54 Å) is the wavelength of incident X-ray. The measured intensities were corrected for absorption and slit smearing effects.[28]

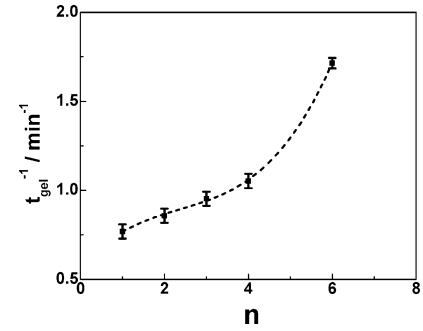

Figure 1. Gelation rate as a function of aliphatic chain length (n) of diesters at 40 °C for polymer concentration 10% (w/v). The dashed line is a guide to the eye.

Dynamic Mechanical Characterization. The storage moduli, loss moduli, and complex viscosities were measured as a function of frequency for 10 wt % PVDF gels in representative DMP and DBP phthalates. Experiments were performed on Rheologica (model: Nova) using parallel plate geometry (25 mm) at 40 °C, keeping the strain amplitude of 0.05 to maintain linear response of the sample. The measured angular frequency, ω, for the oscillatory shear experiment was kept in the range from 0.5 to 700 rad/s. Steady shear experiment was performed for PVDF gels as a function of time at constant shear rate $\gamma = 0.1\ s^{-1}$.

Results and Discussion

Rate of Gelation. The gelation time (t_{get}) and kinetics were measured for PVDF gels in various phthalates at 40 °C. Gelation rates, t_{get}^{-1}, measured for a particular PVDF concentration of 10% (w/v), increase with increasing aliphatic chain length, n, of diesters (Figure 1) primarily because of enhanced interaction with higher aliphatic chain length phthalates. Similar increasing tendency is observed for other concentrations as well in the same temperature. The gelation rate decreases with decreasing PVDF concentration and increasing temperature of gelation. The trend of increasing gelation rate was observed up to $n = 6$ (DHP), and gelation does not occur in higher homologue of phthalates, for example, DOP ($n = 8$). This indicates a solvent dependency phenomenon, where the basic nature of the solvent is same.[15] The theoretical calculation has also been shown the similar order of interaction between polymer and solvent molecules, which increases systematically up to $n = 6$, followed by a sharp decreasing nature.[22] The critical gelation concentrations, below which gelation cannot take place, also follow the similar trend (cf. increases with increasing n).

Solvent Retention and Networking of Gels. Solvent retention power of PVDF gels of 10% (w/v) in various phthalates has been shown in Figure 2. Two-step degradation has been noticed for all solvents. The first step begins after 150 °C, owing to the loss of solvent present in gel, and is also confirmed from ∼90% weight loss corresponding to the solvent in this step. The phenomenon is directly related to the solvent retention power of gel under thermal treatment. Interestingly, the weight loss occurs at higher temperature for gels of higher homologue

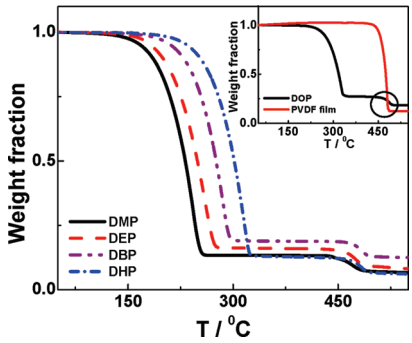

Figure 2. TGA thermograms of the PVDF gels in various phthalates as solvent.

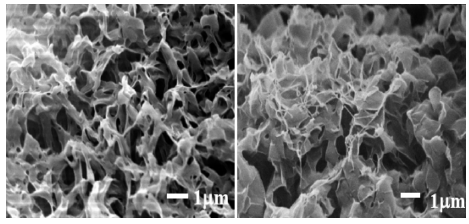

Figure 3. SEM micrographs for dried PVDF gels in DMP (left) and DHP (right) solvents.

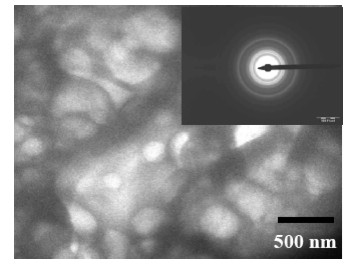

Figure 4. TEM micrographs for dried PVDF gel in DMP.

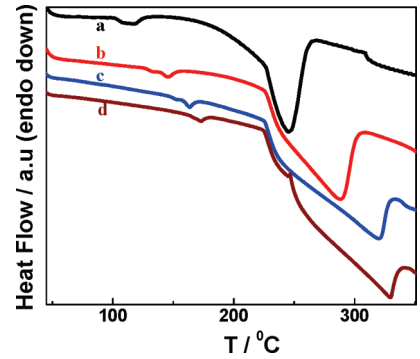

Figure 5. DTA thermograms of the PVDF gels in (a) DMP, (b) DBP, (c) DHP, and (d) DOP solvents.

of phthalates, or, in other words, solvent retention power increases with increasing aliphatic chain length of phthalates. The solvent loss occurs at 160, 183, 205, and 240 °C for gels with DMP ($n = 1$), DEP ($n = 2$), DBP ($n = 4$), and DHP ($n = 6$) solvents, respectively, the same order of increasing gelation rate (Figure 1). The solvent retention power of gel is a measure of interaction between solvent and polymer. Here it has to be mentioned that evaporation/weight loss of a solvent is not related to its boiling point, as evident from the boiling points of DBP ($n = 4$) and DHP ($n = 6$), 340 and 210 °C, respectively. In the case of DHP, weight loss occurs at an even higher temperature than the boiling point of the solvent, presumably due to enhanced interaction between polymer and polar solvent. Hence, the stronger interaction is reflected both in gelation rate and solvent retention power and increases with increasing aliphatic chain length of diesters. Better interaction leading to greater solvent resistance of carboxyethyl chitosan hydrogel modified with hydroxyethyl methacrylate has been demonstrated.[31] The second degradation point at ~450 °C is due to polymer (PVDF) decomposition, which again increases with increasing n. The decomposition temperatures are 450, 455, 467, and 470 °C in DMP, DEP, DBP, and DHP, respectively. After the evaporation of solvent from the gel, the remnants are polymers with various morphologies arising from different gels. The two extreme fibrillar morphologies in solvents with $n = 1$ and 6 have been presented in Figure 3. The fibril dimensions, diameter, and length decrease gradually with increasing n. The thicker and wider distribution of fibrils in lower homologues becomes gradually thinner and narrowly disseminated in higher homologues of phthalates.[22]

The average fibril diameters are 300, 200, 80, and 50 nm for DMP, DEP, DBP, and DHP, respectively. As previously mentioned, enhanced interaction constructs compact and strong fibrils for higher homologue of phthalates, causing higher degradation temperature of gels with higher n diester.

The fibrilar morphology is also evident from the TEM image of dried gel (Figure 4), and the inset shows the electron diffraction pattern indicating α-crystalline structure. However, the dimension of fibrillar morphology is mainly responsible for the varying degradation temperature of gel. It has to be noted here that both solid PVDF film and DOP−PVDF system, which does not form gel, as evident from the flocculation of tiny crystals after some time of dissolution, exhibit the same degradation temperature of ~460 °C, characteristics of PVDF degradation (inset of Figure 2). Therefore, thermal degradation of PVDF with compact and thin fibrillar morphology occurs at 10 °C higher temperature (470 °C) than that of bulk PVDF (~460 °C).

DTA thermograms of gels in various phthalates have been shown in Figure 5. The strong peaks at higher temperature are related to evaporation of solvent from corresponding gels. The peak positions appeared from the inflection point and thereby show higher temperature than that of the degradation temperature calculated from 5% weight loss of solvent (discussed before) but maintain the relative temperature of weight loss. Comparatively weaker endothermic peaks in between 100 and 200 °C indicate gel melting, which increases with aliphatic chain length of diesters. The gel melting temperatures are 116, 145, 163, and 173 °C for DMP, DBP, DHP, and DOP, respectively. The reason for higher melting may lie on the organized and perfect crystallites for higher homologues phthalates, as evident from morphological and kinetic studies. DOP-based semisolid material shows the same melting temperatures as that of solid PVDF film (173.5 °C) because the natures of crystallites are similar in nature. The heats of fusion of gel melting are 3.6, 4.0, 4.9, and 5.3 $J \cdot gm^{-1}$ for DMP, DEP, DBP, and DHP, respectively, and higher values for rising n are attributed to the greater number of crystallites formed for higher n phthalates. Apparently, the double melting endotherms are due to a different type of crystallite present in the gel and is further discussed in the Differential Scanning Calorimetry section.

Gel Formation and Melting. The gel melting behavior in various phthalates has been presented in Figure 6. Interestingly, the gel melting increases systematically with increasing aliphatic chain length. Usually, PVDF shows double melting endotherms, but in gels, it might be due to two different kinds of crystallites present in the gel phase, apparently shown in morphology. The

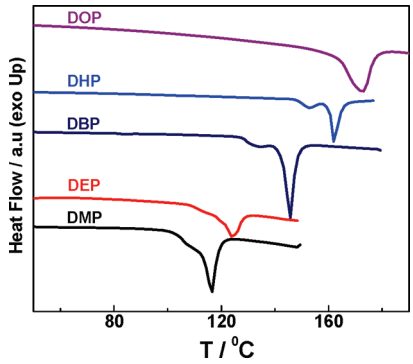

Figure 6. DSC thermographs PVDF gels prepared in indicated phthalate solvents. The heating rate was at 10 °C min^{-1}.

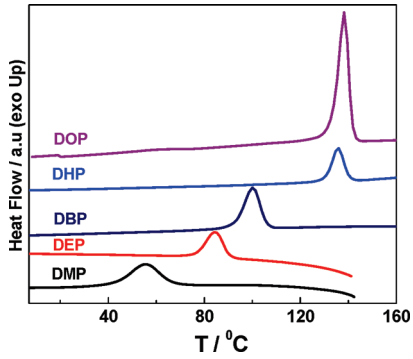

Figure 7. DSC thermographs of PVDF gels prepared in indicated phthalates. The cooling rate was at 10 °C min^{-1}.

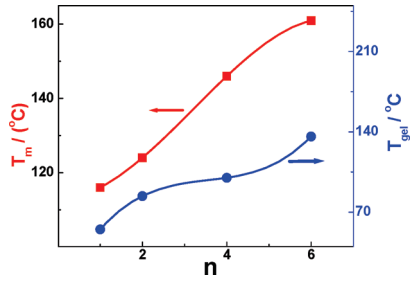

Figure 8. The gel melting, T_m, and the gelation temperature, T_{gel}, under controlled cooling as a function of aliphatic chain length of phthalates n.

lower endotherm is due to melting of crystallites embedded in amorphous zone giving a weak peak, whereas the prominent peaks are due to the discrete crystallites present in the gel phase. It is worth mentioning that low temperature peaks are getting bigger with higher aliphatic chain length, showing a greater number of crystallites embedded in amorphous phase, which is quite obvious from their SEM micrographs. The transformations of sol to gel under controlled cooling have been shown in Figure 7. Here the gel formation occurs at higher temperature for higher aliphatic chain length phthalates. This behavior indicates the relative rate of gel formation as a function of aliphatic chain length. The melting (T_m) and gelation temperature (T_{gel}) against aliphatic chain length have been plotted in Figure 8, exhibiting increasing order of both T_m and T_{gel} with increasing n. The higher melting temperatures in higher n phthalates suggest that ordered and thicker crystallites are formed for higher aliphatic chain length phthalate. Increasing order of temperature of fusion and gelation with increasing n has been observed for aliphatic diesters with varying intermittent chain length.[15] Crystallite formation is easier in higher n phthalates, and the same results are obtained in gelation kinetics. The heat of fusion (ΔH_m) of

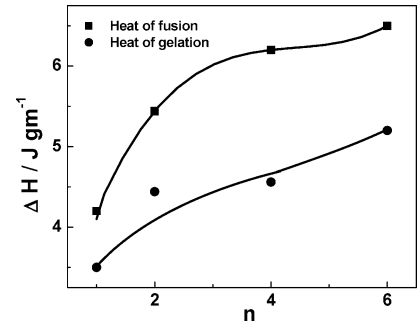

Figure 9. Heat of fusion of gels (ΔH_m) and the heat of gelation (ΔH_{gel}) for 10% (w/v) as a function of aliphatic chain length of phthalates n.

gel and enthalpy of gelation (ΔH_{gel}) have been plotted in Figure 9, revealing increasing tendency with increasing n. This clearly suggests that the absolute crystallinity is higher for higher n phthalates, but in the gel phase, there is significant lowering of melting temperature due to interactions. To understand the interaction between PVDF and phthalates and compound formation thereof, we studied the phase diagram in different phthalates.

The heat of fusion of gel is higher as compared with the heat of gelation for every solvent and is attributed to the considerable amount of ordering after the gel formation and different undercooling for various gels. Furthermore, the gap between two enthalpy values increases with increasing n as a result of ordered crystallites originating from enhanced interaction with high n phthalates for thermodynamic reasons.

Thermodynamics and Compound Formation. The enthalpy of fusion of PVDF gels in different phthalates has been plotted in Figure 10 with the weight fraction of polymer in gels. In the case of DOP, where gelation does not take place, all heat of fusion values lie on the line connecting heat of fusion of pure PVDF and solvent, and ΔH follows the linear rule. It has to be mentioned that solvent does not have any heat of fusion in the temperature range studied here. However, other phthalates, where gelation occurs, exhibit a position deviation from the linearity, indicating the formation of a compound of polymer−solvent complexes. We calculate the heat of fusion of the compound formed during gelation by the equation

$$\Delta H - w_{PVDF}\Delta H_{PVDF} = \Delta H_{comp} \quad (1)$$

Obviously, the measured heat of enthalpy (ΔH) is the summation of the heat of fusion of PVDF in that weight fraction plus the ΔH of compound formed in gels. The positive deviation does show the formation of compound up to DHP ($n = 6$). Apparently, the peak of the deviation gradually shifts to lower PVDF weight fraction with increasing n. Furthermore, the composition of the compound was measured from the peak of the plot of ΔH_{comp} as a function of weight fraction of PVDF (Figure 11). Interestingly, the composition of the compound formed gradually shifts to lower weight fraction of PVDF with increasing n. The values are 0.7, 0.6, 0.57, and 0.5 for DMP, DEP, DBP, and DHP, respectively. These values are corresponding to the molar ratio of the monomeric units of PVDF and phthalate as 7:1, 6:1, and 5:1 for DMP, DEP, and DHP, respectively. The compound formation occurs through the complexation of PVDF and phthalates presumably due to dipole−dipole interaction of the >C═O group of phthalates and >CF_2 group of PVDF molecules. However, the molar ratio of

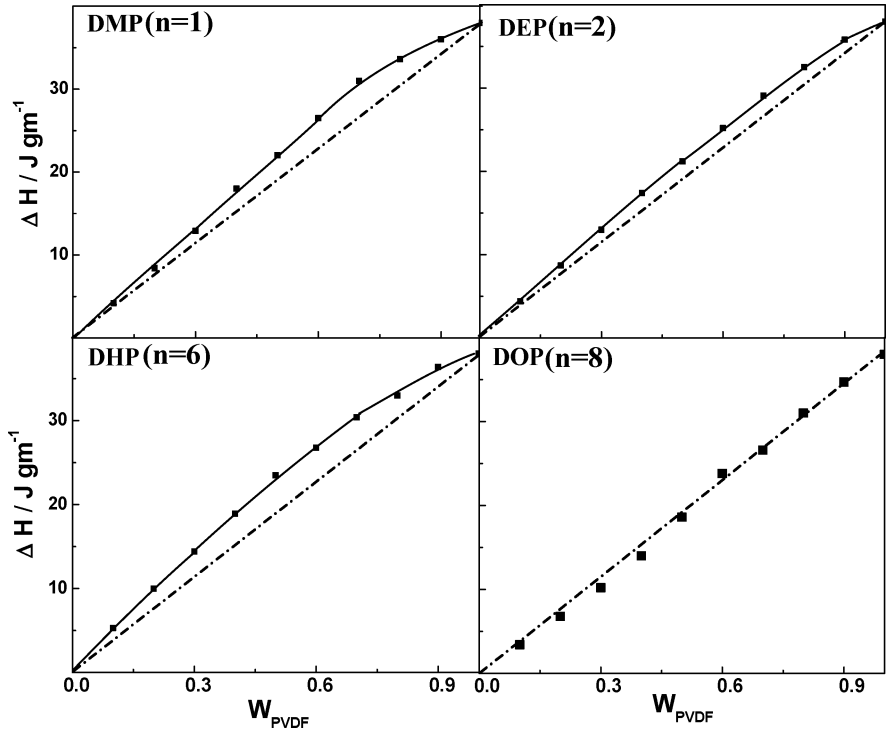

Figure 10. Plot of enthalpy changes during the gel melting process of PVDF in phthalate gels versus weight fraction of PVDF.

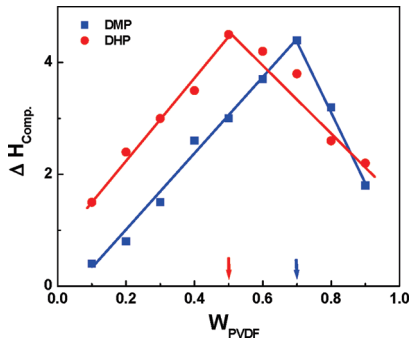

Figure 11. Representative plots for the heat of fusion of compounds (polymer−solvent complexes) versus weight fraction of PVDF gel in DMP and DHP solvents.

VF_2 unit per phthalate molecule gradually decreases with increasing n as a result of better interaction between PVDF and higher homologue of phthalates, which also supports the gelation rate and mechanism. Aliphatic diester with varying intermittent chain length[15] does not show any systematic shift in compound composition as phthalate, and the reason may lie on the gelation kinetics and dynamics of gelation in two different cases. Furthermore, the molar ratio of PVDF monomer unit per solvent molecule is comparatively high (5 to 7 in number) for phthalates as compared with 2 to 3 in number for aliphatic diesters. We have shown that the complex formed from the various trans forms of phthalates and double-strand α-PVDF corroborate the experimental observation through semiempirical electronic structure calculation.[22] To have the double-stranded structure, usually the PVDF chains are slightly puckered and oriented in two different directions to accommodate the bulky phthalates; as a result, the shortest distance between two interactive dipoles is high (∼3.5 Å), as compared with aliphatic diesters (∼2.5 Å). Dikshit et al.[15] show one-by-one layered patterns of PVDF chain and aliphatic diester through MMX calculation, which has to be the ideal close-packed structure of PVDF and aliphatic diester solvent. Hence, the number of monomeric units of PVDF in the compound and dipolar distance, responsible as interacting site, are less in aliphatic diesters as compared with aromatic diesters because of varying interaction in two different systems. However, there is a definite formation of polymer−solvent complexes in phthalates, and the compound composition systematically shifts to lower molar ratio of VF_2 monomer per solvent molecules with increasing aliphatic chain length of phthalates. Because the interaction for higher homologue of phthalates with PVDF is high, a smaller number of VF_2 monomer units is required to form the complex having higher aliphatic chain length phthalate.

Figure 12 shows the phase diagrams of the gels in indicated solvent. Both the gel melting temperature (T_m) and the gelation temperature (T_{gel}) have been plotted with weight fraction of PVDF in gel. In the case of pure PVDF, these are the melting temperature and the crystallization temperature, respectively. Deconvoluted DSC endotherms (Figure S1 of the Supporting Information) clearly show two melting peaks, and we have taken the major peak here. The phase diagram considering both thermal events has been shown in Figures S2 and S3 of the Supporting Information. The nature of the curves for T_m and T_{gel} is almost same, but there is a split of ∼30 °C. It may arise because of the hysteresis effect of the first-order transition and also because of the use of finite heating/cooling rates. Systems where the phase diagrams obtained on cooling and on heating are very similar can be regarded as being formed under equilibrium.[15,16] Therefore, the phase diagrams may be considered to be of the polymer solvent systems formed under equilibrium. In the case of DOP, which does not form gel, both of the temperature curves are parallel to the x axis, showing independent melting and crystallization temperature irrespective of weight fraction of PVDF. Here instead of gel, small crystallites are visible even in naked eye for any concentration of PVDF, which offers crystallization temperature (lower curve) during cooling, and its melting corresponds to the upper curve. There is no depression of melting point exhibiting noninteracting nature of PVDF and DOP. Both T_m and T_{gel} gradually decrease

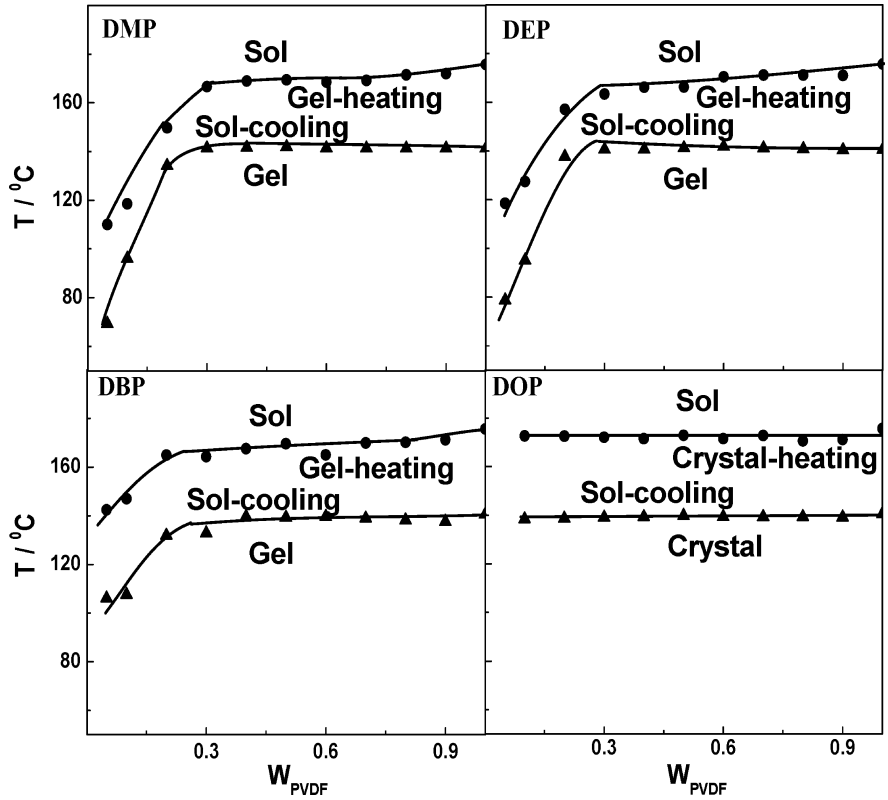

Figure 12. Gel melting temperature and gelation temperature versus weight fraction of PVDF in gel in indicated solvents.

with decreasing PVDF content up to 30 wt %, followed by a steep decrease up to 5 wt % or minimum concentration, where gelation can occur, of polymer for all phthalates other than DOP. This decreasing tendency does show the interacting nature of PVDF and phthalates up to $n = 6$. As per the composition of polymer−solvent complexes, 7, 6, and 5 monomeric vinylidene fluoride groups are associated with every phthalate molecule in DMP, DEP, and DHP, respectively. Therefore, 7/1, 6/1, and 5/1 ratios of monomeric unit of PVDF/solvent (DMP, DEP, and DHP phthalate, respectively) make an interaction site. The number of interaction site per solvent molecule is very high for higher w_{PVDF}, revealing that most of the sites are unable to form a complex, resulting in a meager depression of gel melting and gelation temperature. On the contrary, at lower w_{PVDF}, the interacting sites per phthalate drastically decrease, causing greater interaction from the greater number of contact points, and hence gel melting and gelation temperature decrease steeply. However, the effect of compound formation on the phase diagram and aliphatic chain length of phthalates has been conferred, showing differences in gelation behavior in phthalates with varying n. It has to be remembered here that the extent of dipolar interaction between PVDF and phthalates increases with increasing n as the distance between the dipole decreases with increasing n.[22]

The increasing tendency to form stronger compound for higher homologue of phthalates has been shown in Figure 13. The ΔH_{comp} (heat of fusion of compound) gradually increases for higher homologue of phthalates. We calculated the enthalpy of the compound from the deviation from linearity by using eq 1, which is again almost the same as that measured from the heat of fusion of the first peak in DSC, believed to be due to the heat of fusion of corresponding compound (Figure 13). Therefore, the aromatic diester has an advantage over its aliphatic counterpart that the heat of compound formation systematically increases with n.

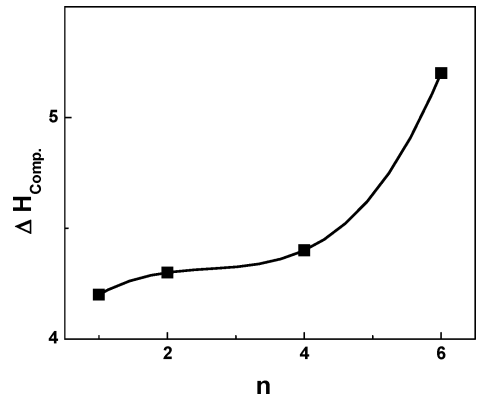

Figure 13. Heat of fusion of compound formed from polymer−solvent complexes in different PVDF−phthalate gels as a function of aliphatic chain length, n.

Small Angle X-ray Scattering. To understand the insight into the typical morphology, SAXS has been measured for dried gels. The SAXS scattering profiles of three representative dried gels have been shown in Figure 14 on a double logarithmic scale. The initial linear behavior of the profiles indicates that the SAXS profiles follow the power-law behavior ($I(q) \approx q^{-\alpha}$) over a wide q range, where $I(q)$ is the scattered intensity and q is the wavevector. The value of α would be 4.0 for smooth surface of the scattering objects following Porod's law. Non-integer values for α indicate the fractal nature. For mass fractals with dimension D_m, $\alpha = D_m \leq 3$, whereas for surface fractals with dimension D_s, $\alpha = (6 - D_s) > 3.0$ and $2 \leq D_s \leq 3$. Therefore, the slope of the scattering curve on the log−log scale indicates the type of fractal. Detailed discussion of fractals is given in the literature.[29,30] The slope of the lines for all gels is found to be ~3.8, indicating a surface fractal nature with a fractal dimension. Usually, the power-law scattering is observed in a limited q range determined by upper and lower cut-off

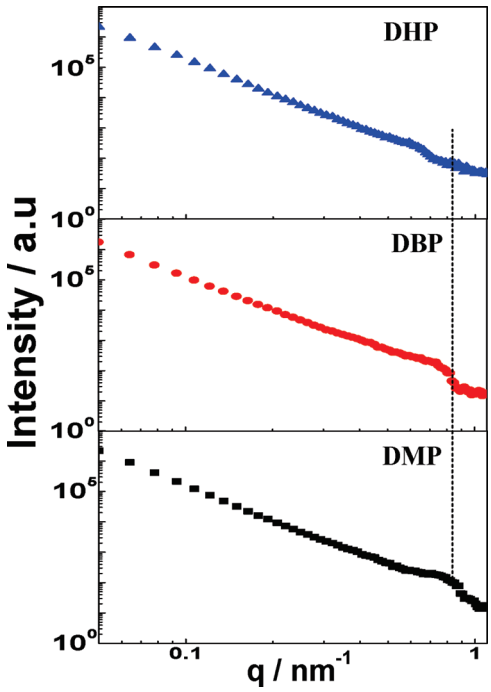

Figure 14. Small-angle X-ray scattering intensity $I(q)$ of PVDF dried gels prepared from indicated solvents. The deviation of the peak position has been shown by vertical dashed line.

SCHEME 1[a]

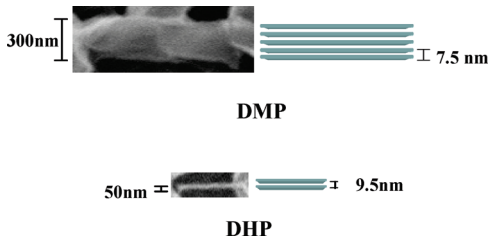

[a] Left part has been taken from an isolated fibril of SEM images of gels for DMP ($n = 1$) and DHP ($n = 6$). The schematic representation of lamellar organization (right portion) constitutes individual fibril with dimension in gels with DMP and DHP solvent.

length scales, between which the system behaves as a fractal. SAXS results suggest that the samples contain the high density polymers, which might be the crystalline fibrils and voids with a rough interface for the interfibrillar region. This is also supported by the morphology of the dried gels in different phthalates (Figures 3 and 4). Interestingly, the scattering patterns show a peak, and the peak position gradually shifts toward lower wavevector region with increasing aliphatic chain length of solvent. The peaks in the scattering patterns indicate the lamellar morphology, and the characteristic lengths ($\Lambda_c = 2\pi/q_m$, calculated from Bragg's equation, where q_m is the wavevector corresponding to peak maxima) are 7.5, 7.7, 8.7, and 9.5 nm for DMP, DEP, DBP, and DHP, respectively. The interlamellar spacings are nearly equal in magnitude, as measured using small-angle neutron scattering data of PVDF dried gels.[22] The calculated average numbers of lamellae in individual fibril, as measured from fibril diameter and Λ_c, are 40, 26, 9, and 5 for DMP, DEP, DBP, and DHP, respectively (Scheme 1). Therefore, a greater number of lamella is required to form a fibril for lower homologue of phthalates because of less interaction. A smaller number of lamella can form a fibril for better interacting higher n phthalates. Therefore, there is a gradual change of assembly of lamellae in one fibril depending on the extent of interaction between polymer and various phthalates and that may be noticeable in mechanical properties of gels as well. However, SAXS data reveal the internal lamellar structure of fibrils of gel with varying aliphatic chain length. The correspondence between the observed morphology and lamellar structure with exact dimension has been presented in Scheme 1 for representative DMP and DHP gels. A similar hump/peak in SAXS patterns was observed in the ι-carrageenan[32] surfactant system because of the gel−micellar system involving ordered nanoorganization (shrinkage or collapse gel) in the presence of surfactant.

To show the changes in structure of gel and dried gel, SAXS experiment has been conducted with gel samples in presence of respective phthalates. The SAXS profiles of the wet gels plotted on log−log scale are shown in Figure 15. The data in the low q region (I) arise from the structure of larger inhomogeneities. These may be due the concentrated and dilute regions formed as a result of phase separation in the gels.[25] The profiles in this region follow a power law $I(q) \approx q^{-m}$. The value of the exponent m varies between 2 and 3, indicating a mass fractal nature of the concentrated regions formed in the framework of dilute (amorphous) gel and solvent. However, because of the limitations in the accessible lower q range of our machine, a limited portion of this region is visible in the data. As the samples are dried (in dried gels), the mass fractal nature transforms to a surface fractal (the exponent varies between 3 and 4, Figure 14) because of the evaporation of solvent leaving a clear void and polymer-rich regions with fractally rough interfaces between them. It may be noticed that the lower limit (q_l) of the fractal region, representing the basic building blocks of the fractals, extends to much higher q after the gels are dried with $q_l \approx 0.08$ nm^{-1} for the wet gels to $q_l \approx 0.7$ nm^{-1} for dried gels.

Interestingly, the curves at high-q regions (II) differ significantly for wet and dried gels. In the wet gels, a humplike feature in the region $0.08 < q < 0.6$ nm^{-1} indicates aggregation or precipitation of polymer crystallites present in the high-dense regions in the medium of weak amorphous polymer chains and voids. The data in this region were fitted to the function $I(q) = I(o)/[1+ (\xi q)^2]^{-\alpha/2}$, where $\alpha = 4$ for smooth surface of the scatterers and ξ is the correlation length.[33] For $\alpha \neq 4$, this function can be modified[34−36] with ξ proportional to the average radius of the aggregates. The fitted profiles have been shown in the Figures, and the parameters are listed in Table 1. The values of $\alpha > 4$ indicate a diffuse or fuzzy boundary between the aggregates and the surrounding matrix.[27] The plateau region at further high-q region (III) could be arising from randomly distributed micropores of size <10 nm formed in solvent and gel matrix. As the gels are dried and the solution gets evaporated, a small correlation peak appears in this region (Figure 14) for dried gels, suggesting the formation of ordered structure within the concentrated polymer-rich phase due to the correlated rearrangement of solid particles.

Rheological Studies

Dynamic Mechanical Properties. The frequency dependence storage modulus, $G'(\omega)$, loss modulus, $G''(\omega)$, and complex viscosity, $\eta^*(\omega)$, in dynamic mode of PVDF representative gels were measured at 40 °C and have been presented in Figure 16a−c. $G'(\omega)$ is greater than $G''(\omega)$ over the entire range of ω, and both moduli are almost constant at lower frequency range up to 60 rad s^{-1}, indicating an apparent steady-state gel. Interestingly, both the storage and loss modulus decrease with increasing aliphatic chain length n. Moreover, a significant dip in storage and loss modulus is prominent, followed by its rising

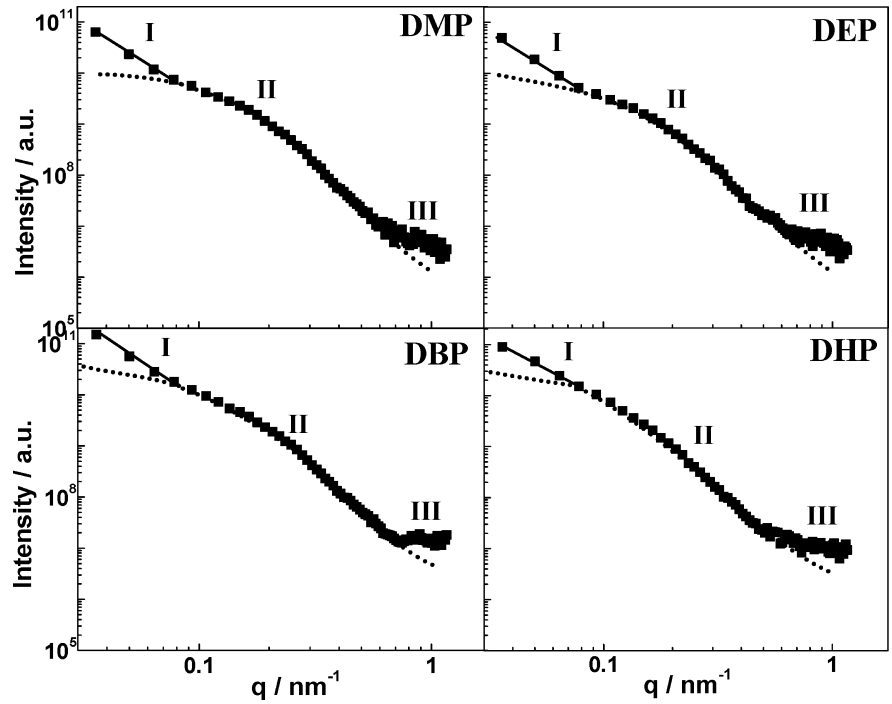

Figure 15. Small-angle X-ray scattering intensity $I(q)$ of PVDF gels (10 wt % in the presence of solvent) prepared from indicated solvents. The different zones have been indicated for various structures, as mentioned in the text. The solid and dotted lines represent the fitting curves, and the points are experimental data.

TABLE 1: Parameters Obtained by Fitting the SAXS Data of Wet Gels in the Regions I and II

sample	m	ξ (nm)	α
DMP	2.9	7.0	4.8
DEP	2.8	7.5	4.8
DBP	2.7	8.0	4.6
DHP	2.3	10.5	4.7

tendency with increasing frequency. The similar dip is also observed in complex viscosity of PVDF gel in both phthalates. The dipping of moduli and viscosity is presumably due to the disordering of structure, which was previously formed during gelation in the form of crystallites/fibrils. The subsequent increase in modulus and viscosity is primarily due to the reformation of the structure by reorienting crystallites/fibril at higher frequency. It is noteworthy to mention here that disordering starts at a particular frequency depending on the strength of the ordered structure (fibrils), which starts at lower frequency for higher homologue of phthalates because of thinner fibril dimension. The dip starts at 100 rad s^{-1} for DMP system, whereas it begins at 60 rad s^{-1} for DBP system. The explanation of higher mechanical properties of lower homologue of phthalates is pertinent mainly because of thicker fibril dimension (cf. Figure 3 and SAXS discussion). The disordering and ordering phenomena in the second run as well strongly suggests the reversible nature of order−disorder type of transition in gels. These observations are anomalous to the previous reports[20,37] where semisolid behavior is clear but does not exhibit any dip, presumably because of the absence of order−disorder transition. Dynamic measurements of pluronic poly(acrylic acid) hydrogel exhibit this kind of dip in moduli and tan δ curves, of which the initial frequency of dip gradually increases with increasing concentration of polymer in gels.[38] Therefore, it is obvious that order−disorder transition is exhibited in aromatic diesters, whereas it is categorically absent in aliphatic diesters. The moderate interaction between PVDF−phthalate (less than aliphatic diesters, as evident from higher dipole−dipole distance in aromatic systems) leads to such crystallites whose order−disordered transition is observable in the measurable frequency range, whereas a similar phenomena was not observed for aliphatic diesters.

Steady Shear Viscosity. The shear viscosity in the steady-state measurement of PVDF gels has been shown in Figure 17. The viscosity of gels with lower homologue of phthalates exhibits higher viscosity, indicating similar nature, as in case of dynamic behavior. Furthermore, the viscosities are constant over a longer period of time, showing the performance of normal polymer melts where there is no change of structure during deformation. Most probably, the shearing effect is not sufficient to promote disordering−ordering phenomena at lower shear rate ($\gamma = 0.1$ s^{-1}). The measurement of steady shear has also been checked at higher shear rate, showing lowering of viscosity at higher time, but flowing ability is so high that samples flow out of plate. However, the relative order of viscosity is similar both in dynamic and static shear experiment and decreases with increasing aliphatic chain length of phthalates originating from the varying dimension of fibril in their respective morphologies.

Therefore, the solvent retention power, microstructure, morphology, mechanical properties, scattering patterns, and their origin and thermodynamic phase diagram of PVDF−phthalates have been illustrated, and the properties of polymer−solvent gel pairs can be predicted to be of similar interacting nature.

Conclusions

Solvent retention power of PVDF gels has been reported in a series of homologous aromatic diesters (phthalates), and it increases with aliphatic chain length of diester where the extent of interaction gradually increases. Thermal degradation of gels strongly depends on its morphology, and thermal stability increases for compact crystallites and higher crystalline gels where interactions between the components are significant. The fibrils are ordered and organized for higher n phthalates, even though they are thinner in nature, as evident from SEM images.

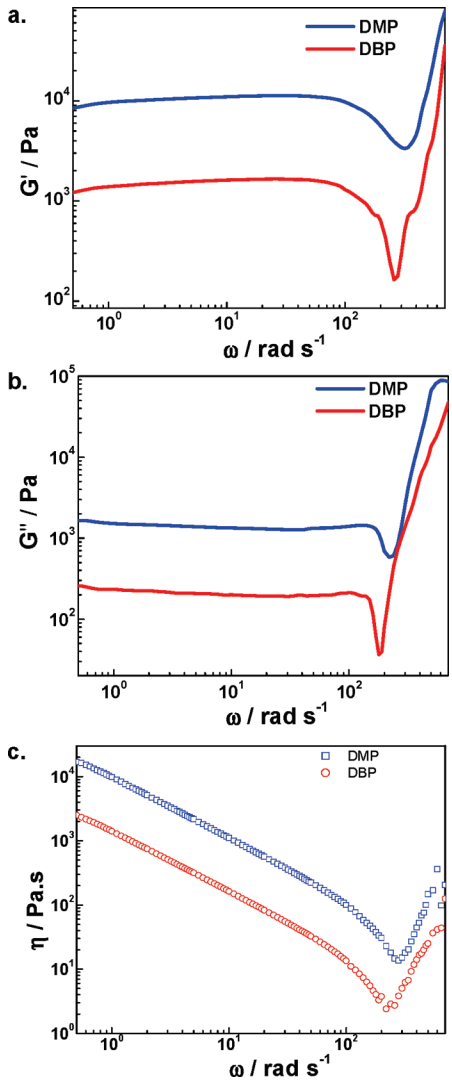

Figure 16. Mechanical responses of PVDF−phthalate gels in dynamic mode: (a) storage modulus (G'), (b) loss modulus (G''), and (c) viscosity (η^*) of PVDF gels (10% (w/v)) from indicated solvents at 40 °C.

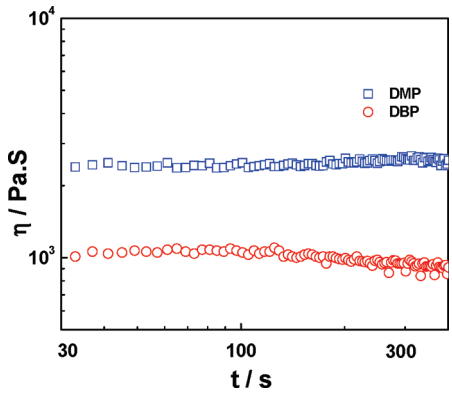

Figure 17. Steady shear viscosity (η) versus time of PVDF gels (10% w/v)) prepared from DMP and DBP solvents at 40 °C ($\gamma = 0.1$ s^{-1}).

The gel melting and gelation temperatures increase with increasing aliphatic chain length of phthalates. The enthalpy of gel melting shows a positive deviation from linearity exhibiting compound formation, where gelation occurs, indicating the formation of polymer−solvent compound. DOP, where gelation does not occur, shows good linearity with respect to weight fraction of PVDF. A systematic change (decreasing polymer content) of compound composition has also been observed with increasing aliphatic chain length of phthalates. SAXS profiles follow the power law behavior, and the patterns indicate the fractal geometry in gels. The appearance of hump in the scattering patterns suggests the lamellar organization inside the fibril, and the interlamellar distance increases with aliphatic chain length. The semisolid behavior of gels has been manifested in the rheological behavior at lower frequency range, whereas splintering of network structure, followed by its reformation or order−disorder transition, took place at the high-frequency region depending on the strength of fibrillar morphology. Steady shear experiment also confirms the relative strength of gel similar to dynamic measurement, and the storage modulus is higher for lower aliphatic chain length of phthalates in existence of thicker fibrils in gels.

Acknowledgment. We acknowledge the receipt of research grant from UGC-DAE CSR, Mumbai Centre (project no. CSR/CD/MUM/CRS-M-116). The supply of PVDF samples from Ausimont, Italy is gratefully acknowledged. We also acknowledge Dr. M. Yashpal and Prof. G. Singh, IMS, BHU, for TEM studies.

Supporting Information Available: Deconvolution of DSC peaks by fitting the original DSC thermograms and gel first and minor melting temperature, second and major melting temperature, and gelation temperature versus weight fraction of PVDF in gels. This material is available free of charge via the Internet at http://pubs.acs.org.

References and Notes

(1) Reinecke, H; Mijangos, C; Brulet, A; Guenet, J. M. *Macromolecules* **1997**, *30*, 959.
(2) Daniel, C.; Menellet, A.; Brulett, A; Guenet, J. M. *Polymer* **1997**, *28*, 4193.
(3) Guenet, J. M.; McKenna, G. B. *Macromolecules* **1988**, *21*, 1752.
(4) Fazel, N.; brulet, A; Guenet, J. M. *Macromolecules* **1994**, *27*, 3836.
(5) Poux, S.; Malik, S.; Thierry, M; Guenet, J. M. *Polymer* **2006**, *47*, 5596.
(6) Babin, H.; Dickinson, E. *Food Hydrocolloids* **2001**, *15*, 271.
(7) Dahmani, M.; Ramzi, J; Rochas, C.; Guenet, J. M. *J. Colloid Interface Sci.* **2003**, *31*, 147.
(8) Tanigami, T.; Suzuki, H.; Yamaura, K.; Matsuzawa, S. *Macromolecules* **1985**, *18*, 259.
(9) He, X.; Herz, J.; Guenet, J. M. *Macromoleeules* **1987**, *20*, 2003.
(10) Ray, B.; Elhasri, S.; Thierry, A.; Marie, P.; Guenet, J. M. *Macromolecules* **2002**, *35*, 9730.
(11) Ramzi, M.; Rochas, C.; Guenet, J. M. *Macromolecules* **1996**, *29*, 4668.
(12) Saiani, A.; Spevacek, J.; Guenet, J. M. *Macromolecules* **1998**, *31*, 703.
(13) Cho, J. W.; Song, H. Y.; Kim, S. Y. *Polymer* **1993**, *34*, 1024.
(14) Mal, S.; Maiti, P.; Nandi, A. K. *Macromolecules* **1995**, *28*, 2371.
(15) Dikshit, A. K.; Nandi, A. K. *Macromolecules* **2000**, *33*, 2616.
(16) Dixit, A. K.; Jana, T.; Malik, S.; Nandi, A. K. *Polym. Int.* **2003**, *52*, 925.
(17) Dasgupta, D.; Manna, S.; Malik, S.; Rochas, C.; Guenet, J. M.; Nandi, A. K. *Macromolecules* **2005**, *38*, 5602.
(18) He, Y.; Lodge, T. P. *Macromolecules* **2008**, *41*, 167.
(19) Stokke, B. T.; Draget, K. I.; Smidsrod, O.; Yuguchi, Y.; Urakawa, H.; Kajiwara, K *Macromolecules* **2000**, *33*, 1853.
(20) Dasgupta, D.; Manna, S.; Garai, A.; Dawn, A.; Roches, C.; Guenet, J. M.; Nandi, A. K. *Macromolecules* **2008**, *41*, 779.
(21) Yadav, P. J. P.; Aswal, V. K.; Sastry, P. U.; Patra, A. K.; Maiti, P *J. Phys. Chem. B* **2009**, *113*, 13516.
(22) Yadav, P. J. P.; Ghosh, G.; Maiti, B.; Aswal, V. K.; Goyal, P. S.; Maiti, P. *J. Phys. Chem. B* **2008**, *112*, 4594.
(23) *Thermoreversible Gelation of Polymers and Biopolymers*; Guenet, J. M., Ed.; Academic Press: London, 1997.
(24) Shinohara, Y.; Kayashima, K.; Okumura, Y.; Zhao, C.; Ito, K.; Amemiya, A. *Macromolecules* **2006**, *39*, 7386.
(25) Kanaya, T.; Ohkura, M.; Takeshita, H.; Kaji, K.; Furusaka, M.; Yamaoka, H.; Wignal, G. D. *Macromolecules* **1995**, *28*, 3168.

(26) Higgins, J. S.; Benoit; H. C. *Polymers and Neutron Scattering*; Clarendon Press: Oxford, U.K., 1994.

(27) Schmidt, P. W.; Anvir, D.; Levy, D.; Hohr, A.; Steiner, M.; Röll, A. *J. Chem. Phys.* **1991**, *94*, 1474.

(28) Schmidt, P. W.; Height, R. *Acta Crystallogr.* **1960**, *13*, 480.

(29) Schmidt, P. W. *J. Appl. Crystallogr.* **1991**, *24*, 414.

(30) Martin, J. E.; Hurd, A. J. *J. Appl. Crystallogr.* **1987**, *20*, 61.

(31) Zhou, Y.; Yang, D.; Gao, X.; Chen, X.; Xu, X.; Xu, Q.; Lu, F.; Nie, J. *Carbohydr. Polym.* **2009**, *75*, 293.

(32) Shtykova, E.; Dembo, A.; Makhaeva, E.; Khokhlov, A.; Evmenenko, G.; Reynaers, H. *Langmuir* **2000**, *16*, 5284.

(33) Debye, P.; Anderson, H. R., Jr.; Brumberger, H. *J. Appl. Phys.* **1957**, *28*, 679.

(34) Emmerling, A.; Petricevic, R.; Beck, A.; Wang, P.; Scheller, H.; Fricke, J. *J. Non-Cryst. Solids* **1995**, *185*, 240.

(35) Shibayama, M.; Kurokawa, H.; Nomura, S.; Muthukumar, M.; Stein, R. S.; Roy, S. *Polymer* **1992**, *33*, 2883.

(36) Hudson, S. D.; Hutter, J. L.; Nieh, M. P.; Pencer, J.; Million, L. E.; Wan, W. J. *Chem. Phys.* **2009**, *130*, 34903.

(37) Tiitu, M.; Hiekkataipale, P.; Hartikainen, J.; Makela, T.; Ikkala, O. *Macromolecules* **2002**, *35*, 5212.

(38) Broomberg, L. *Macromolecules* **1998**, *31*, 6148.

JP105018H